Chin. J. Astron. Astrophys. Vol. 3 (2003), No. 6, 505–512
(http://www.chjaa.org or http://chjaa.bao.ac.cn)

Chinese Journal of
Astronomy and
Astrophysics

The Two Mini-lobes of the CSO OQ208 — VLBI Observations at 5 GHz and 8.4 GHz *

Wei-Hua Wang, Xiao-Yu Hong and Tao An

Shanghai Astronomical Observatory, Chinese Academy of Sciences, Shanghai 200030;
whwang@center.shao.ac.cn
National Astronomical Observatories, Chinese Academy of Sciences, Beijing 100012

Received 2003 April 23; accepted 2003 June 27

Abstract We present the results of VLBI observations at 5 GHz and 8.4 GHz of the compact symmetric object (CSO) OQ208. Images taken on four epochs at 5 GHz and one at 8.4 GHz show that the parsec radio structure of the source consists of two mini-lobes, both of them are resolved into two hot-spots. We note that the component D is stronger than the component C in the south-west region at 5 GHz, indicating that component D is less free-free absorbed than C at low frequency. On the basis of the separation of components A and D, a proper motion of 0.032 ± 0.02 mas yr^{-1} between the two mini-lobes is estimated. This value is about half the previous estimates based on the separation of components A and C with 8.4 GHz VLBI data. The reason for the decrease in the expansion velocity is discussed.

Key words: galaxies: individual (Mkn 668, OQ208) — galaxies: active

1 INTRODUCTION

GHz-peaked-spectrum (GPS) radio sources are extremely powerful ($L_{\rm radio} \approx 10^{45}\,{\rm erg\ s^{-1}}$) and very compact (10–100 mas, 10–1000 parsecs) sources. They are characterized by a convex radio spectrum peaking around 1 GHz (O'Dea et al. 1991; O'Dea & Baum 1997). GPS radio sources with galaxies tend to show a compact double morphology on parsec scale which were named Compact Symmetric Object (CSOs) (Wilkinson et al. 1994; Stanghellini et al. 1997b, 1999).

Currently, there are three main hypotheses to explain the GPS radio sources and their possible evolution. In the young source scenario, GPS radio sources with compact double (CD) morphology or CSOs represent the very first stage of classical double radio sources (Phillips & Mutel 1982). Owsianik & Conway (1998) and Owisianik et al. (1998) detected the proper motion of the outer edges in CSOs, with an estimated dynamical age of the order of 10^3 years, thus to support this scenario (also see in Liu et al. 2000; Fanti et al. 1995; Fanti 2000). In the

* Supported by the National Natural Science Foundation of China.

second scenario, GPS radio sources will never become as large as the classical doubles since they are confined to the sub-kpc scale by a dense and turbulent ambient medium (O'Dea et al. 1991; Carvalho 1994, 1998). However, it remains unclear about the gas density and its distribution in the nuclear region. The recurrent activity scenario has been proposed to explain the detection of arc-second scale faint extended emission around $\sim 10\%$ of GPS sources (Baum et al. 1990); Stanghellini et al. 1990, 1998). In this hypothesis, the relic of the past activity is still present while the reborn radio source digs its way through the near-nuclear ISM.

OQ208 (J1404+2827) is a compact radio source associated with the bright galaxy Mkn668 of $m_r = 14.6$ (Stanghellini et al. 1993) at $z = 0.077$ (Burbidge & Strittmatter 1972). It is one of the closest bright GPS galaxies, with a convex radio spectrum peaking at about 5 GHz (Stanghellini et al. 1998). This source has been classified as a Seyfert I galaxy. On the basis of its strong radio emission, the source was suggested to be a Broad Line Radio Galaxy (BLRG) (Marziani et al. 1993; Stanghellini et al. 1997a).

The first published VLBI image of OQ208 showed the radio structure to be extended in the N–S direction (Charlot 1990). Zhang et al. (1994) found it to extend 6 mas at position angle $\sim -145°$. The observed morphological structure was interpreted as a typical core-jet of a compact flat-spectrum radio source (Zhang et al. 1994; also see in Bondi et al. 1994). Later VLBI observations showed that OQ208 consists of two mini-lobes with a flux density ratio of about 10 : 1, and a project total size less than 10 pc, both the mini-lobes are resolved into two hot-spots (Stanghellini et al. 1997a; Liu et al. 2000, 2002a). Based on the mas morphology and the spectral information obtained from multifrequency VLA observations, Stanghellini et al. (1997a) suggested OQ208 to be a CSO. The 15 GHz VLBI observations revealed a weak core located between the two mini-lobes and confirmed that OQ208 is a CSO (Kellermann et al. 1998; Stanghellini et al. 2001). Liu et al. (2000) detected a proper motion of 0.058 ± 0.038 mas year^{-1} between the mini-lobes from multiepoch VLBI observation at 8.4 GHz, corresponding to a projected jet speed of $0.095 \pm 0.062c$ ($H_0 = 100$ km s^{-1}Mpc^{-1}, $q_0 = 0.5$, and throughout the rest of this paper). They considered OQ208 to be a young CSOs with a kinematic age of 320 ± 210 years.

In this paper, we present the results of VLBI observations at five epochs, conducted with the EVN (European VLBI Network) at 5 GHz and the VLBA (Very Long Baseline Array) at 8.4 GHz. The proper motion between the two mini-lobes are estimated based on the 5 GHz VLBI data.

2 OBSERVATION AND DATA PROCESSING

The VLBI observations were carried out with EVN on 1997 February 21, 1997 June 10, 1997 November 7 and 1999 June 19 in snapshot mode at 5 GHz. OQ208 was used as a calibrator in all four observations, and was observed about 3–6 scans every 13 minutes. The antennas involved in each observation are listed in Table 1.

The data were obtained with the MK III mode B recording system (28 MHz bandwidth). The correlation process was performed in Bonn with the Max Plank Institut für Radionastronomie MK III correlator with 4 second integration time.

In addition, we also acquired VLBI data of OQ208 at 8.4 GHz from the radio reference frame image database (RRFID) (http://rorf.usno.navy.mil/rrfid.shtml). The antennas involved are listed in Table 1. Detailed information can be seen in the RRFID homepage.

The primary data reduction of the VLBI data, including editing, amplitude calibration and fringe fitting, was done by the NRAO Astronomical Imaging Processing Software (AIPS) package (Cotton 1995; Diamond 1995). Post-processing including editing, phase and amplitude self-calibration, and imaging of the data, was performed with AIPS or the package DIFMAP (Shepherd et al. 1994). The final images were displayed using AIPS.

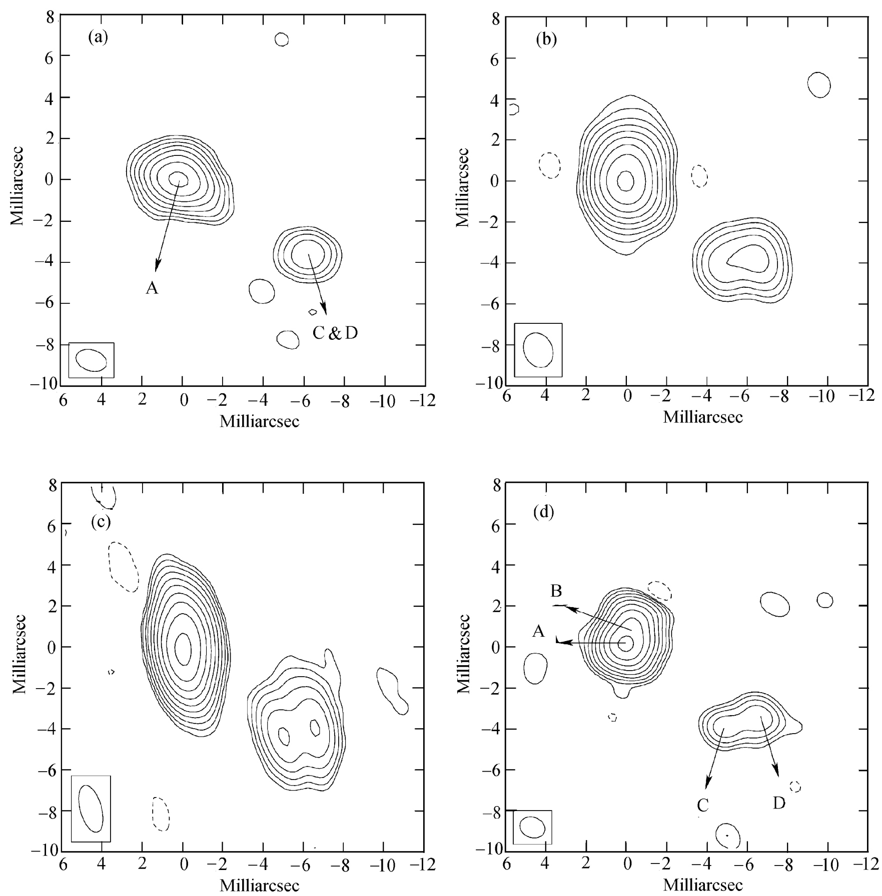

Fig. 1 VLBI images of OQ208 at 5 GHz at epochs 1997.14 (a); 1997.44 (b); 1997.85 (c); 1999.13 (d). Peak flux densities are 1.08, 1.47, 1.27, and 0.83, the rms noise values are 2.3, 1.6, 0.6, and 0.9 mJy beam^{-1}, and the lowest contours are 7.0, 5.0, 2.0, and 2.7 mJy beam^{-1}, respectively. Contour levels increase by a factor of 2 each step. The restoring beam in each image is shown by the ellipse in the lower-left corner. The parameters in each image are also seen in Table 1.

The images obtained at the various epochs at 5 GHz are presented in Fig. 1. The image for the epoch 1998.48 at 8.4 GHz is presented in Fig. 2. The peak flux density, the levels of the contours and the information of the restoring beam are also listed in Table 1. In each image the lowest contour level is three times the off-source rms noise level, the contour levels are increased by a factor of 2 each step, and the beam size is shown by the ellipse in the lower-left corner, and listed in Table 1.

Table 1 Telescopes used in the Observations and the Parameters of the Images in Figs. 1 and 2

Epoch	Antennas [a]	$S_{\rm peak}$ [b] (Jy/b)	Contours [c] (mJy/b)	Restoring Beam [d] Maj×Min	P.A.
1997.14	Ef, Sh, Cm, Jb, Mc, On, Hh, Tr, Wb	1.08	7.0×(−1, 1, 2, . . ., 256)	1.54×1.01	73.73
1997.44	Ef, Sh, Ur, Jb, Mc, Cr, Nt, Hh, Tr	1.47	5.0×(−1, 1, 2, . . ., 256)	1.75×1.40	26.65
1997.85	Ef, Sh, Ur, Jb, Mc, Cr, Nt, On, Hh, Tr, Wb	1.27	2.0×(−1, 1, 2, . . ., 256)	2.36×1.06	15.98
1999.13	Ef, Sh, Ur, Cm, Jb, Mc, Nt, On, Hh, Wb	0.83	2.7×(−1, 1, 2,. . ., 256)	1.28×0.99	70.97
1998.48	Mc, On, Ny, Gc, Kk, Gn, Wf, VLBA	0.96	7.0×(−1, 1, 2, . . ., 256)	1.67×0.58	–4.18

[a] Antenna codes: Ef: Effelsberg, Sh: Shanghai, Ur: Urumqi, Cm: Cambridge, Jb: Jodrell Bank (MK2), Mc: Medicina, Cr: Crimea, Nt: Noto, On: Onsala, Hh: Hartebeesthoek, Tr: Torun, Wb: WSRT, Ny: Nyales20, Gc: Gilcreek, Kk: Kokee, Gn: Nrao20, Wf: Westford; VLBA: all 10 antennas

[b] the peak brightness

[c] the lowest contour level and contours level

[d] the size and position angle of the restoring beam: Maj×Min (mas), P.A.(°)

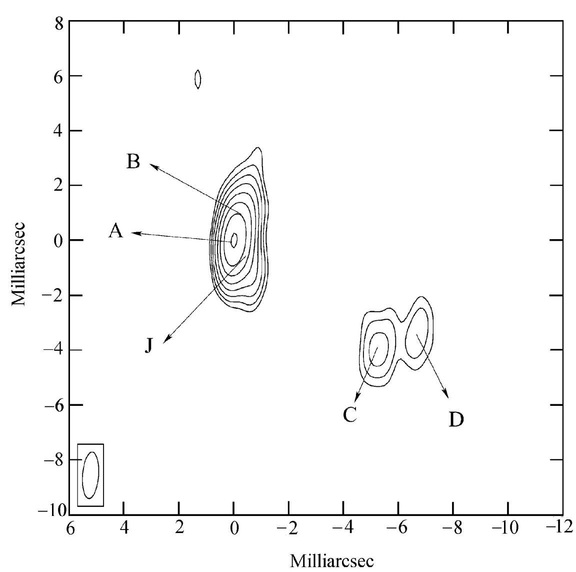

Fig. 2 VLBI images of OQ208 at 8 GHz for the epoch 1998.48. The peak flux density is 0.96, the rms noise value is 2.2 mJy beam^{-1}, and the lowest contour is 7.0 mJy beam^{-1}. Contour levels are increased by a factor of 2 each step. The parameters in each image are also given in Table 1.

3 AN ANALYSIS OF THE IMAGES

Our observations at all epochs (Fig. 1) show the radio structure of the source at 5 GHz to consist of two mini-lobes. The two mini-lobes are resolved into two components, which are assumed to be the two hot-spots of the radio source, in the three images except the one on epoch 1997.14. This is consistent with the previous images and models available in literature (Stanghellini et al. 1997a; Liu et al. 2000, 2002a). The components are labelled A, B, C and D as shown in Fig. 1 (d), following the convention of Stanghellini et al. (1997a). Component A is the strongest one. Furthermore, we detect a new component at P.A. $-151.2°$ from the strongest component A at 8.4 GHz. It is labelled J (Fig. 2). We find that, compared to the component C, the component D is stronger in the south-west region at 5 GHz, and is weaker in the VLBI observation at 8.4 GHz and higher frequencies (e.g. Fig 2. in this paper; Liu et al. 2000; Kellermann et al. 1998). This indicates that the component C is more free-free absorbed than component D at low frequencies.

To obtain a qualitative picture of the morphology of OQ208, we tried to fit the calibrated visibility of each images with Gaussian models with the MODELFIT program in the DIFMAP. The brightest component is fitted by an elliptical Gaussian component, and the other components , with circular Gaussian components. The results are listed in Table 2, where we also list the models available at the same frequency on epoch 1993.1 (Stanghellini et al. 1997a). The columns in Table 2 are as follows: Col. 1 is the observation epoch; Col. 2, the component label; Col. 3, the flux density of each component; Cols. 4 and 5, the distance and position angle with respect to the strongest component A; Cols. 6, 7 and 8 are the parameters of the Gaussian model: the width at half maximum, the axis ratio and the orientation of the individual component. The uncertainties of position are estimated considering the various possible models from the different methods and the formulae given by Fomalont (1999). The errors of position are assumed to be 0.1 mas.

Table 2 Results of Model Fitting at 5 GHz

Obs. inf	Comp.	Flux (mJy)	R (mas)	Θ (°)	θ_M (mas)	Ratio	pa (°)
(1)	(2)	(3)	(4)	(5)	(6)	(7)	(8)
1993.10	A	1250.0	0.0	0.0			1.2
	B	1090.0	1.30	–14.0			1.7
	C	100.0	6.50	–121.0			2.2
	D	110.0	7.40	–117.0			0.8
1997.14	A	1893.2	0.0	0.0	1.31	0.75	81.5
	C&D	151.5	7.40	–120.4	1.14	1.0	–45.0
1997.44	A	2053.0	0.0	0.0	1.08	0.89	–16.7
	B	254.8	1.29	–16.8	0.51	1.0	6.3
	C	72.5	6.15	–129.0	0.68	1.0	18.4
	D	163.3	7.60	–118.4	0.86	1.0	4.4
1997.85	A	1444.0	0.0	0.0	0.96	0.67	–22.1
	B	641.6	1.27	–15.7	0.79	1.0	36.9
	C	98.9	6.42	–127.5	0.99	1.0	35.5
	D	93.8	7.53	–118.0	0.68	1.0	–6.3
1999.13	A	1365.6	0.0	0.0	1.02	0.65	–24.8
	B	326.6	1.25	–20.1	0.51	1.0	11.3
	C	31.3	6.30	–129.3	0.43	1.0	26.6
	D	80.3	7.59	–119.6	0.82	1.0	31.0
1998.48	A	990.5	0.0	0.0	0.39	0.55	–66.7
	B	261.1	0.93	–27.8	0.57	1.0	23.2
	J	189.7	0.73	–151.2	0.82	1.0	14.0
	C	70.3	6.62	–127.4	0.64	1.0	35.5
	D	41.0	7.54	–115.8	0.47	1.0	13.0

At 8.4 GHz and higher frequencies, the component C is the stronger component in the south-west region (Liu et al. 2000; Kellermann et al. 1998; Stanghellini et al. 2001). Liu et al. (2000) estimated the relative motions between the two mini-lobes based on the separation of components A and C over a period of 41 months. Similarly we also detect the separation between the two mini-lobes from the components A and D at 5 GHz, over a period of about 63 months. In Fig. 3, we plot the separation between the two components A and D vs. epoch for each epoch at 5 GHz reported in Table 2. We also plot the one for epoch 1998.48 at 8.4 GHz with a triangle. From Fig. 3, a rate of separation of 0.032 ± 0.02 mas yr^{-1} between components A and D was estimated, which corresponds to an actual jet velocity of $0.074 \pm 0.046c$. The velocity is about one-half of the previous estimate by Liu et al. (2000) at 8.4 GHz. The separation between the two hot-spots A and B in the north-east region is constant from our results. Due to its large uncertainty resulting from its weaker flux density, the relative velocity between C and D in the south-west region is hard to define. Based on the model-fitting result (See Table 2), a flux density ratio between the two mini-lobes of about 12:1 was estimated.

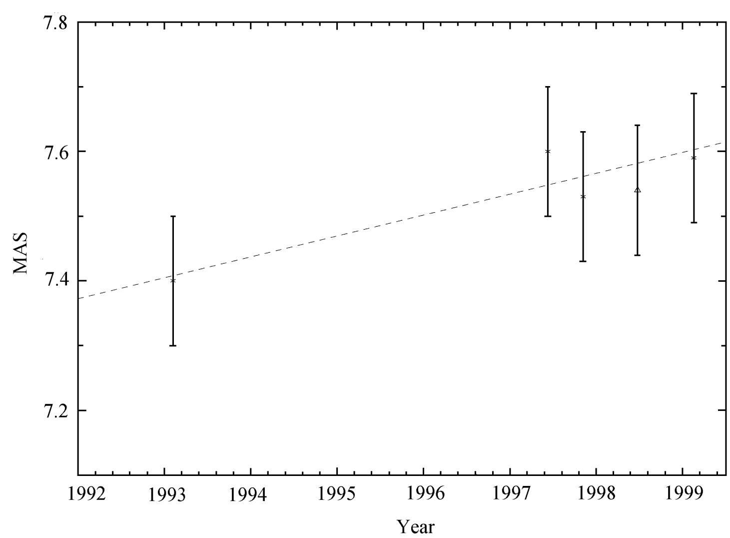

Fig. 3 Separation versus time for components A and D.

4 DISCUSSION AND CONCLUSIONS

Based on the model-fitting results of C and D at 5 GHz at epoch 1999.13 and at 8.4 GHz at epoch 1998.48, the spectral index between 5 GHz and 8.4 GHz is estimated. The index of the component C is 1.56 and that of the component D is –1.34. The inner component C has a flatter spectrum than the outer component D. The young source scenario indicates that two-sided jets are emitted from the central core to form double lobes at the end. The overall structure is buried in the ambient plasma. Along the line of sight inclined to the jet axis, the optical depth towards the receding jets will be thicker than the advancing jets. Therefore the receding jets are strongly free-free absorbed. The asymmetric free-free absorption (FFA) successfully interpret the large flux ratio between two mini-lobes of OQ208 at low frequency (Kameno et al. 2000). According to the asymmetric FFA the component D should be strongly free-free absorbed. This is inconsistent with our results that the component C is more strongly free-free absorbed than component D. We consider that the electron density is larger around the nuclear region than in the outer region and therefore the component C is more free-free absorbed than D at low frequency. The free-free absorption is of no effect at higher frequencies, so there, the component C is the brighter one.

We detect proper motion between A and D on the basis of VLBI observations at 5 GHz at four epochs. The value is smaller than what was estimated on the basis of 8.4 GHz VLBI observations (Liu et al. 2000). One possibility is that the position of the jet components depends on the observed frequency. On the other hand, the velocity of the two hot-spots are different. This means the proper motion slowed down. The decrease of expansion speed is possibly due to the shocked ambient medium on the front. The detection of the hot-spot separation velocity provides an age below 10^4 year for the CSOs. This is an important piece of evidence to support the young source scenario. If the speed of expansion really becomes slow, the age of CSOs we estimated will have larger uncertainty. The ambient medium in the nuclear region must be considered.

Acknowledgements This research was supported by the National Natural Science Foundation of China (19973103). W. H. Wang thanks Dr. Liu Xiang for valuable discussion and Dr. Chen Ding for help on the paper. The European VLBI Network is a joint facility of European, Chinese, South African and other radio astronomy institutes funded by their national research councils. The Very Long Baseline Array is a facility of the National Radio Astronomy Observatory, operated by Associated Universities, under cooperative agreement with the National Science Foundation. This research has made use of Radio Reference Frame Image Database of the United States Naval Observatory. This work has made use of NASA Astrophysics Data System Abstract Service.

References

Baum S. A., O'Dea C. P., Murphy D. W. et al., 1990, A&A, 232, 19

Bondi M., Mantovani F., Sherwood W. et al., 1994, A&AS, 103, 365

Burbidge E. M., Strittmatter P. A., 1972, ApJ, 172, L37

Carvalho J. C., 1994, A&A, 292, 392

Carvalho J. C., 1998, A&A, 329, 845

Charlot P., 1990, A&A, 229, 51

Cotton W. D., 1995, In: J. A. Zensus, P. J. Diamond, P. J. Napier, eds., Very Long Baseline Interferometry and the VLBA. ASP Conference Series 82, 189

Dallacasa D., Fanti C., Fanti R. et al., 1995, A&A, 295, 27

Diamond P. J., 1995, In: J. A. Zensus, P. J. Diamond, P. J. Napier, eds., Very Long Baseline Interferometry and the VLBA. ASP Conference Series 82, 227

Fanti C., Fanti R., Dallacasa D. et al., 1995, A&A, 302, 317

Fanti C., In: J. E. Conway, A. G. Polatidis, R. S. Booth, Y. Pihlström, eds., Proceedings of the 5th European VLBI Network Symp., 2000, Published Onsala Space Observatory

Fomalont E. B., 1999, In: G. B. Taylor, C. L. Carilli, R. A. Perley, eds., Synthesis Imaging in Radio Astronomy II, p. 301

Kameno S., Horiuchi S., Shen Z. Q. et al., 2000, PASJ, 52, 209

Kellermann K. I., Vermeulen R. C., Zensus A. J. et al., 1998, AJ, 115, 1295
Liu X., Stanghellini C., Dallacasa D. et al., 2000, Chin. Phys. Lett., 17(4), 307
Liu X., Stanghellini C., Dallacasa D. et al., 2002, A&A, 385, 768
Liu X., Phd thesis, 2002
Liu X., Yang Jun, 2003, Acta Astronomica Sinica, 44, 296
Marziani P., Sulentic J. W., Calvani M. et al., 1993, ApJ, 410, 56
O'Dea C. P., Baum S. A., Stanghellini C., 1991, ApJ, 380, 66
O'Dea C. P., Baum S. A., 1991, AJ, 112, 1480
Owsianik I., Conway J. E., Polatidis A. G., 1998, A&A, 336, L37
Owsianik I., Conway J. E., 1998, A&A, 337, 69
Phillips R. B., Mutel R. L., 1982, A&A, 106, 21
Shepherd M. C., Pearson T. J., Taylor G. B., 1994, BAAS, 26, 987
Stanghellini C., Baum S. A., O'Dea C. P. et al., 1990, A&A, 233, 379
Stanghellini C., Baum S. A., O'Dea C. P. et al., 1993, ApJ, 88, 1
Stanghellini C., Bondi M., Dallacasa D. et al., 1997a, A&A, 318, 376
Stanghellini C., O'Dea C. P., Dallacasa D. et al., 1997b, A&A, 325, 943
Stanghellini C., O'Dea C. P., Dallacasa D. et al., 1998, A&AS, 131, 303
Stanghellini C., O'Dea C. P., Murphy D. W. et al., 1999, A&AS, 134, 303
Stanghellini C., Dallacasa D., O'Dea C. P. et al., 2001, A&A, 377, 377
Wilkinson P. N., Polatidis A. G., Readhead A. C. S. et al., 1994 ApJ, 432, L87
Zhang F. J., Bath L. B., Spencer R. E., 1994, A&A, 281, 649